Journal of Materials Chemistry B

COMMUNICATION

View Article Online
View Journal | View Issue

Cite this: J. Mater. Chem. B, 2015, 3, 738

Received 6th October 2014
Accepted 12th December 2014

DOI: 10.1039/c4tb01646g

www.rsc.org/MaterialsB

Cation–π interaction in DOPA-deficient mussel adhesive protein mfp-1†

Sangsik Kim,‡[a] Ali Faghihnejad,‡[b] Yongjin Lee,‡[c] YongSeok Jho,*[c] Hongbo Zeng*[b] and Dong Soo Hwang*[a]

Here we report the possible contribution of cation–π interaction to underwater adhesion of mussels by using DOPA-deficient recombinant mussel adhesive proteins. Considering the instability of DOPA in an oxidative environment, the cation–π interaction in DOPA-deficient biopolymers provides a complementary cross-linking mechanism for the design of novel underwater adhesives.

Currently, one of the most challenging issues faced by medical and dental industries is introducing and maintaining strong adhesion on polar surfaces in the presence of moisture. In the case of medical adhesives, the target surfaces are hydrated with body fluids. However, most commercial adhesives cannot be applied to such wet surfaces because of the loss of adhesion strength and the side effects caused by the constituent toxic chemicals. In contrast, in natural environments, marine mussels effectively adhere to wet substrates *via* various adhesion mechanisms.[1] Over the past decade, there has been increasing interest in adhesive systems of marine mussels (*e.g.*, *Mytilus* species) as sources of potential biomedical underwater adhesives.[1a,2]

Mussels survive in the turbulent intertidal zones of the ocean by robust tethering to wave-swept substrata *via* a proteinaceous holdfast; this is the so-called byssus.[3] The byssus is a group of byssal threads secreted by the mussel foot, and it can dissipate the mechanical stress exerted from tides and buoyancy. At the end of the byssal thread, there is an adhesive plaque where actual underwater adhesion occurs. Individual byssal threads of mussels are mainly composed of approximately 20–30 different types of proteins. The proteins involved in the mussel underwater adhesion are named mussel foot proteins (mfps) or conventionally called mussel adhesive proteins. So far, 6 types of mfps have been identified and characterized (mfp-1 to 6).[2b] All mfps contain 3,4-dihydroxyphenyl-L-alanine (DOPA), which is a catecholic amino acid post-translationally modified from tyrosine.[2a,c] DOPA is known to play a key role in the mussel underwater adhesion by bonding with a variety of molecules, including biomacromolecules, polymers, metal ions, and metal oxides.[2] However, DOPA has a propensity to be oxidized in the presence of oxygen or in neutral and basic pHs, consequently losing its adhesion ability.[3] Therefore, complementary strategies to prevent the oxidation of DOPA have been proposed.[4] Recent nanomechanical studies on mussel adhesive proteins suggest another key underwater adhesion mechanism: cation–π interaction.[5]

Cation–π interaction, which occurs between an electron-rich π system (*e.g.*, Tyr, Dopa, Phe, Trp) and the adjacent cations (*e.g.*, n-terminus amine, Lys, Arg, His),[6] is a non-covalent interaction, whose strength is comparable to that of hydrogen bonds and electrostatic bonds in the aqueous phase.[6] Cation–π interactions in living organisms play critical roles in various physiological activities, including potassium channel blocking,[7] nicotinic acetylcholine (ACh) signal transmission,[8] numerous protein foldings,[9] and T-cell antigen receptor binding.[10] Recently, strong and reversible underwater cohesions between two films of native mfp-1s were measured; mfp-1s possess bare negatively charged amino acid residues at the pH tested. Cation–π interaction was suggested as one of the underlying mechanisms for the cohesion of mfp-1s, with the fact that mfp-1 has roughly equal amount of phenyl groups (*i.e.*, Tyr, DOPA, Trp) and positively charged groups (mainly Lys).[5] However, the native mfp-1s previously studied contain unknown post-translational modifications (PTMs) and DOPA residues; direct

[a]School of Environmental Science and Engineering, Division of Integrative Biosciences and Biotechnology, Pohang University of Science and Technology, Pohang, Gyeongbuk, 790-784, Korea. E-mail: dshwang@postech.ac.kr; Tel: +82 54 2799505

[b]Department of Chemical and Materials Engineering, University of Alberta, Edmonton, AB, T6G 2V4, Canada. E-mail: hongbo.zeng@ualberta.ca; Tel: +1-780-492-1044

[c]Department of Physics, Pohang University of Science and Technology, Asia Pacific Center for Theoretical Physics, Pohang, Gyeongbuk, 790-784, Korea. E-mail: ysjho@apctp.org

† Electronic supplementary information (ESI) available: Recombinant mussel foot protein-1 (Rmfp-1) and its decapeptide preparation, surface preparation, surface topography using atomic force microscopy (AFM), force measurement by surface forces apparatus (SFA), quantum simulation method, Rmfp-1 conformation. See DOI: 10.1039/c4tb01646g

‡ These authors contributed equally to this work.

nanomechanical measurements on mussel adhesive proteins in the absence of PTMs can help in elucidating the contribution of cation–π interaction to mussel underwater adhesion.[5]

In this work, the nanomechanics of the recombinant *Mytilus* foot protein-1 (Rmfp-1, $(AKPSYPPTYK)_{12}$) and its decapeptide (AKPSYPPTYK) without any PTM were directly probed using a surface forces apparatus (SFA) (Fig. 1). The results indicate that cation–π interaction can be one of the major factors contributing to underwater adhesion of the mussel protein. Such experimental configurations exclude interfering effects and interactions from the post-translational modifications (PTMs) such as reactive DOPA residues in native mussel adhesive proteins. Rmfp-1 was selected as it contains the same amount of tyrosine (π system, 20 mol%) and lysine (cation, 20 mol%); moreover, Rmfp-1 has no negatively charged amino acid residues at the pH of the testing buffer (~3.0). K^+, whose binding affinity to the π structure is stronger than that of Na^+ and Li^+,[6,11] was chosen as a competing cation for the cation–π bonding between Rmfp-1s and decapeptides. Numerical simulations were performed to correlate the experimental results. All atomic-level molecular dynamics[12] were carried out to investigate the molecular conformation of Rmfp-1. In addition, *ab initio* quantum mechanical simulations[13] were conducted to determine the binding energies of cation–π and π–π interactions, both in a water and in a vacuum environment, to elucidate the role and impact of water molecules in cation–π and π–π interactions.

Rmfp-1 (13.6 kDa) was produced from *E. coli*[4d] and the decapeptide of mfp-1 (1.1 kDa) was prepared by trypsin digestion of Rmfp-1. Rmfp-1 and the decapeptide of mfp-1 without any PTM were used lest the interaction be influenced by DOPA, a key functional group for mussel underwater adhesion. Rmfp-1 ($(AKPSYPPTYK)_{12}$) and the decapeptide ($(AKPSYPPTYK)_1$) differ only in their decapeptide repetition numbers. The decapeptide has two positively charged lysine residues and two aromatic tyrosine residues at pH < 9. The interaction forces between a layer of Rmfp-1 or the decapeptide-coated mica and a bare mica surface (asymmetric configuration, Fig. 2A), or those between two Rmfp-1 layers or two decapeptide layers (symmetric configuration, Fig. 2B), were measured using SFA. All the molecular force measurements were performed in 0.1 M acetic acid, pH ~3.0, with the amount of KNO_3 added ranging from 100 μM to 400 mM. Atomic force microscopy (AFM) images of the decapeptide-coated mica and Rmfp-1-coated mica show that the protein films were uniformly deposited on and fully covered the mica surfaces (Fig. S1†). The root-mean-square (RMS) roughness of the decapeptide and Rmfp-1 surfaces was ~0.2 nm and ~0.3 nm, respectively. The AFM images indicate that the Rmfp-1 coated surface was slightly rougher than the decapeptide coated surface.

Fig. S2† shows that when two protein films, decapeptide (closed circle) or Rmfp-1 (open triangle), were kept in contact, the adhesion energy W_{ad} only slightly increased with increasing the contact time from 2 to 40 minutes, indicating that the adhesion between the protein layers could reach a plateau within the 2 minutes of contact. Similar contact time effects

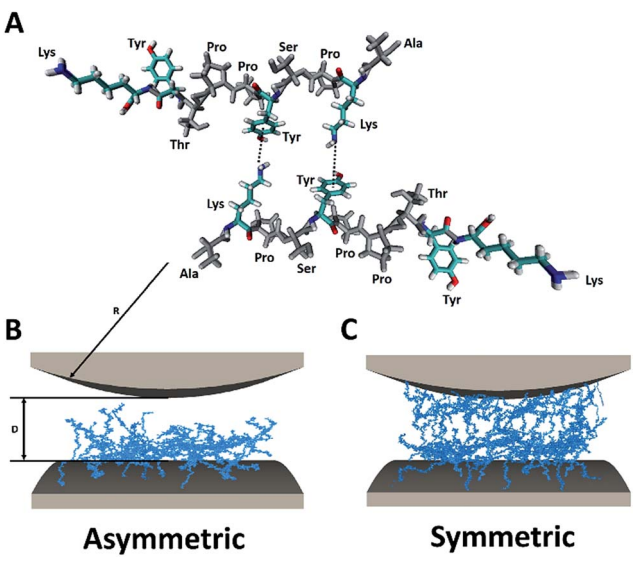

Fig. 1 (A) Schematic of (A) the decapeptide of Rmfp-1 with a polyproline type II helix conformation,[15a,b] (B) asymmetric configuration, (C) symmetric configuration. *R* is the radius of the surfaces and *D* is the distance between two opposing mica surfaces.

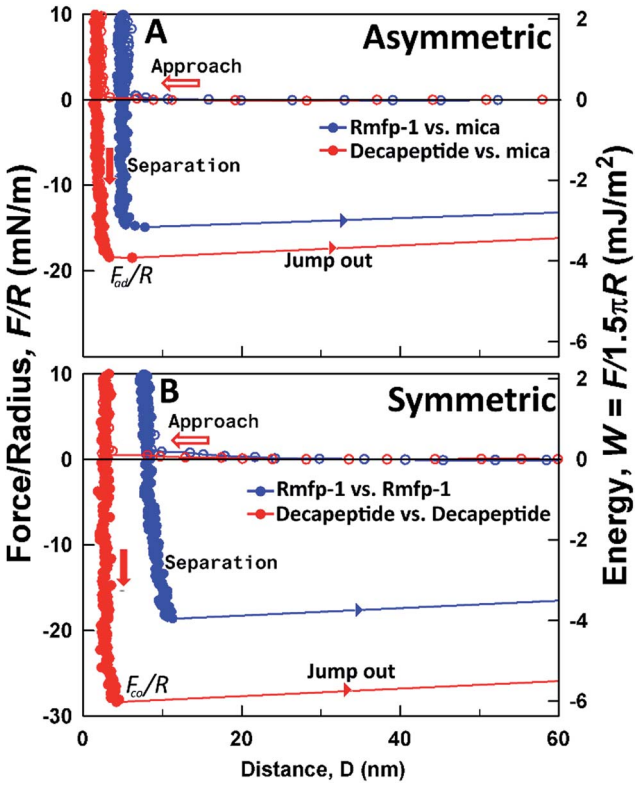

Fig. 2 Force–distance profiles of Rmfp-1 (blue) and decapeptide (red) films on mica. (A) Asymmetric configuration; (B) symmetric configuration. Open circle – approach, closed circle – separation. The measured force, *F*/*R* (normalized by the radius of the surfaces, *R*), is denoted in the ordinate at the left, whereas the corresponding interaction energy per unit area, *W*, between two flat surfaces, defined by $W = F/1.5\pi R$ is on the right. F_{ad} and F_{co} are the adhesion force and cohesion force for the asymmetric and symmetric cases, respectively.

were observed for adhesion between proteins and mica. Therefore the contact time was fixed at 2 min in this study to investigate the impact of salt concentration in the following experiments. It is also noted that the maximum normalized load applied during force measurements was fixed at $F/R \sim 10$ mN m^{-1}.

As shown in the force–distance profiles in Fig. 2, no significant repulsion is detected between the two interacting surfaces for both the symmetric and asymmetric cases during approach because the Debye length, given by $\kappa^{-1} = 0.304/(\sqrt{[KNO_3] + [HAc]})$nm, is less than 1 nm under the solution conditions tested. For the asymmetric case in Fig. 2A, strong adhesions with $F_{ad}/R \sim -14.2$ and -18.2 mN m^{-1} ($W_{ad} \sim 2.2$ mJ m^{-2} and $\sim$2.9 mJ m^{-2}) were detected during separation for Rmfp-1 *vs.* mica, and decapeptide *vs.* mica, respectively. The measured adhesion or "pull-off" force F_{ad} is related to the adhesion energy per unit area W_{ad}, as $F_{ad} = 1.5\pi RW_{ad}$ for soft deformable surfaces with strong adhesive contact.[14] For the asymmetric case, electrostatic attraction between the positively charged Rmfp-1 or decapeptide and the negatively charged mica plays the dominant role in the measured adhesion.

Interestingly, strong cohesions, $F_{co}/R \sim 18$ and 28 mN m^{-1} (or $W_{co} \sim 2.9$ and 4.5 mJ m^{-2}), were also measured between two positively charged Rmfp-1 films and two decapeptide films (symmetric configuration, Fig. 2B), respectively, whose linear charge densities even exceed the Manning threshold (1.26 e nm^{-1}, when fully ionized). These densities also exceed the strength of electrostatic attraction between the positively charged mussel proteins and the negatively charged mica, as shown in Fig. 2A.

One possible electrostatic attraction may be caused by the strong correlation between charged proteins of opposing surfaces, but in this case, the attraction should be significantly weaker than that in the case of the asymmetric configuration. Thus, we can rule out electrostatic interaction as the origin of strong attraction, and attribute this attraction to the cation–π interaction between the tyrosines of one surface and the lysines of the other surface or to π–π stacking between two opposing tyrosines together with other attractive interactions such as van der Waals interaction and hydrogen bonding. In order to evaluate the possible contribution of the π–π stacking, the interaction forces between two poly-L-tyrosine (pTyr) films coated on mica were measured using the SFA under the same buffer conditions (0.1 M acetic acid, pH $\sim$ 3.0). No detectable cohesion was measured between the two pTyr surfaces; this indicates that the π–π stacking is not strong enough to overcome the electrostatic repulsion. Therefore, the strong cohesive interactions between the two Rmfp-1 films and the two decapeptide films are mainly caused by cation–π interactions. Surprisingly, the quadrupole–monopole interaction (cation–π) is stronger than the monopole–monopole interaction (between a cation and an anion), which is counter-intuitive. Indeed, some previous studies have revealed that this remarkable phenomenon can occur in aqueous solution due to the low desolvation penalty of the cation–π interaction.[6,9,11] The cohesive energy W_{co} of $\sim$4.5 mJ m^{-2} measured in the present study is about 30% of the interaction between the strongest DOPA-mediated attraction between mussel adhesive protein and mica (Mefp-5 to mica, $W_{ad} \sim 14$ mJ m^{-2}). Although the DOPA-mediated interaction is stronger than the cation–π interaction in an aqueous environment, DOPA tends to be oxidized, thereby losing its adhesion ability as pH increases.[4a,b] Therefore, exploitation of cation–π interactions can be a complementary strategy to achieve successful underwater adhesion. It is noted that the cohesion between Rmfp-1 films is lower than that between two decapeptides of Rmfp-1 films, which is most likely because the longer Rmfp-1 chains adsorbed on the mica surface have more flexible and random conformations as compared to that of the much shorter decapeptide, as supported by the confined film thickness in SFA force measurements and AFM imaging (Fig. S1†). The more condensed and ordered decapeptide films could facilitate the formation of effective cation–π interaction between the two opposing surfaces that contributes to the stronger cohesion measured.

To further understand the system, the salt effect was investigated by introducing KNO_3. As shown in Fig. 3, the adhesion strength decreases with increasing the interfering cation K^+ concentration for both the Rmfp-1 and the decapeptide cases, which is mainly due to the screening of electrostatic interactions at higher salt concentrations. The increase in salt concentration plays two roles: it screens any electrostatic field

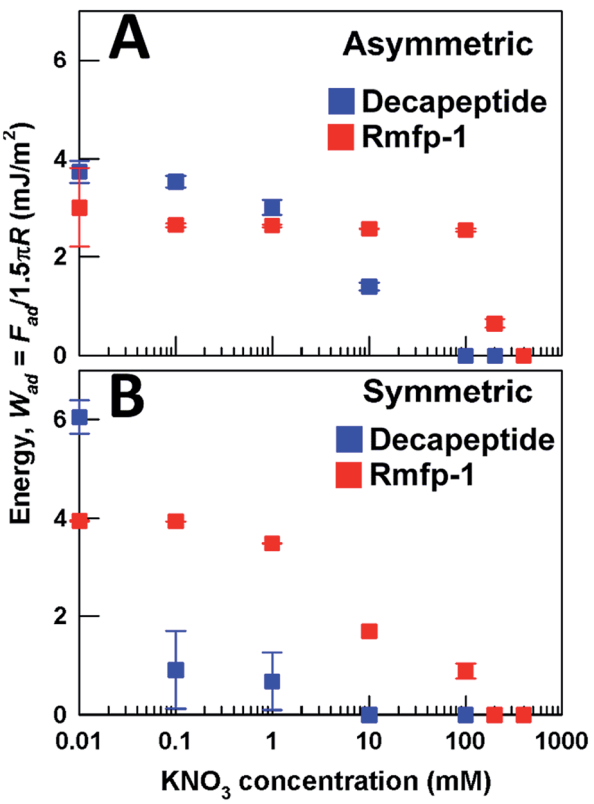

Fig. 3 Dependence of adhesion energy on KNO_3 concentration, W_{ad}. (A) Asymmetric configuration; (B) symmetric configuration. Blue square – decapeptide, red square – Rmfp-1. Each value represents the standard deviation of three independent force runs.

and increases the entropic (and steric) pressure between the two surfaces. Both these phenomena reduce the attraction in the asymmetric case. The respective adhesions of Rmfp-1 to mica and the decapeptide to mica completely disappeared at KNO_3 concentrations of 100 mM and 400 mM, respectively.

As the KNO_3 concentration was increased from 0 to 400 mM, the adhesion between the decapeptide and Rmfp-1 at pH 3.0 (100 mM sodium acetate) gradually weakened, eventually falling to 0 mN m^{-1} at KNO_3 concentrations of 10 mM and 200 mM, respectively.

It should be emphasized that the salt promotes different effects in asymmetric and symmetric systems. In asymmetric systems, the main role of the salt is the reduction of electrostatic interactions. If we use the bare Debye–Huckel approximation, the electrostatic decay length is reduced to about 0.5 nm. In contrast, in a symmetric system, the chaotropic ion, K^+, can replace lysine in the cation–π bond even at low concentrations (~1 mM, Fig. 3). It is known that both K^+ and a positively charged primary amine group of lysine show similar interaction strength with π systems. KNO_3 eventually reduces the electrostatic force in both systems, but the reduction in force is much more sensitive to the increase in KNO_3 concentration in symmetric systems. As the mussel protein layer is positively charged while the mica surface is negatively charged in a buffer solution at pH 3.0, the strong adhesion measured was mainly attributed to the electrostatic attraction.

It is interesting to note that the interaction energy of the decapeptide drops faster than that of Rmfp-1 with increase in the KNO_3 concentration. As the adsorbed decapeptide could have a more ordered conformation due to its much shorter chains than that of Rmfp-1, it is easier for K^+ ions to diffuse to the adsorbed decapeptide layer and interfere with the cation–π interaction between the opposing decapeptide surfaces. Whereas, it is relatively more difficult for K^+ to diffuse into the much thicker Rmfp-1 layer which has a more random and flexible conformation and is less ordered as compared to that of the decapeptide (as confirmed from SFA measurements and AFM imaging), therefore showing a relatively weaker interfering capability to the cation–π interaction (or cohesion) of the two opposing Rmfp-1 surfaces.

The specific interaction of the polymer at the surface can change the surface structure and the consequent interaction, for example the charge steering hydration bond interaction.[15,16a] From computer simulations, it is found that Rmfp-1 adopts a worm-like conformation, which stems from the strong line charge density (1.26 e nm^{-1}) that exceeds the value specified by the Manning threshold, and from the left-handed polyproline type II (PPII) helix of the decapeptide. On the oppositely charged surfaces the polymers are highly correlated with each other and they could be more elongated and aligned. Thus, this may lead to the increase of the packing ratio of Rmfp-1 on the surface, and consequent adhesion (Fig. S4 and S5†).[15,16b,c] The estimated length of the cylinder along the principal axis is about 19.1 nm ± 2.6 nm, and the radius is about 3.1 nm ± 0.41 nm. Indeed, the confined thickness of Rmfp-1 in the SFA is almost the same as the diameter of the Rmfp-1 cylinder, suggesting that Rmfp-1 is very finely coated on the anionic mica surface. The Rmfp-1 cylinders possibly align parallel with one another, as in the case of DNA.[15c] The interspacing between the Rmfp-1s depends on the surface charge density of mica. As a corollary, about 11.3 nm confined thickness between two positively charged Rmfp-1 films in the SFA experiment can be understood (Fig. 2). Next, we calculated the interactions between the two films based on the cation–π interactions. The binding energies of individual cation–π pairs are about -1.30×10^{-20} J in water, and -1.32×10^{-19} J in vacuum. The π–π interaction may contribute to the attraction, but its magnitude is smaller (-7.40×10^{-21} J in water, -3.54×10^{-20} J in vacuum) compared with that of the cation–π interaction. In addition, the π–π interaction is subject to stricter geometrical restrictions than the cation–π interaction; this suggests that the cation–π interaction is the main cause of the strong attraction. Presumably, these are responsible for non-detectable cohesion between the two pTyr-coated surfaces in the SFA experiment (π–π interaction). The maximum charge density that Rmfp-1 can have is approximately 0.22 e nm^{-2}. Since the mica charge density is higher than this maximum, we can approximate the interspace distance of Rmfp-1s as its diameter. In this configuration, the estimated interaction strength is about -2.69τ mJ m^{-2} for water and -27.3τ mJ m^{-2} for vacuum, where τ is the fraction of cation (π) residues participating in the formation of the cation–π bond. It is known that inside the condensed polymer, dehydration occurs. Therefore, the actual solvent conditions and interaction strength should be between those in water and vacuum. Therefore, at least 4 of the 24 cation residues participate in binding when fully dehydrated. If the dehydration is weak, almost all the cation–π bonds should be connected. Thus, the numerical analysis reveals the following: (1) Rmfp-1 is adsorbed on the anionic mica surface, and the Rmfp-1 cylinders are presumably aligned parallel to one another; (2) the adhesion of Rmfp-1s and the decapeptides is quantitatively explained by the cation–π interaction; (3) when two films are in contact, fewer water molecules occupy the interstitial region of tyrosine and lysine, which are involved in the formation of the cation–π bond (Table 1).

It should be noted that other factors such as attractive van der Waals interaction, hydrogen bonding, and polymer conformations also contribute to the strong cohesion measured between two positively charged Rmfp-1 protein films (or two positively charged decapeptide films) with relatively strong electrostatic repulsion (Fig. 2). Introducing and increasing interfering cation K^+ concentration significantly decreases the cohesion measured (Fig. 3), which directly supports that cation–π interactions significantly contribute to the cohesion measured (as the presence of K^+ could not significantly affect

Table 1 Cation–π and π–π interactions in water and vacuum

Interaction type	Solvent	Energy (J)
Cation–π	None (vacuum)	-1.32×10^{-19}
	Water	-1.30×10^{-20}
π–π	None (vacuum)	-3.54×10^{-20}
	Water	-7.40×10^{-21}

the van der Waals interaction and hydrogen bonding that leads to a significant drop of adhesion in Fig. 3, while increasing KNO_3 concentration and screening the electrostatic repulsion between the Rmfp-1 protein films would have led to a stronger attraction). Therefore, the above experimental results and theoretical simulations indicate that cation–π interaction significantly contributes to the adhesion between DOPA-deficient recombinant mussel adhesive proteins.

Conclusions

In summary, we demonstrate that exploiting cation–π interactions can be a complementary strategy for successful underwater adhesion. DOPA is known as a key component in the mussel adhesion but the other unknown key components need to be explored. We measure the possible contribution of the cation–π interaction to mussel adhesion by using DOPA-deficient mussel adhesive proteins (Rmfp-1). Strong cohesion, which is mostly mediated by cation–π interactions between the Rmfp-1 films ($W_{co} \sim 2.9$ mJ m^{-2}) or the decapeptide of Rmfp-1 ($W_{co} \sim 4.5$ mJ m^{-2}), was measured at pH 3.0; the strength of these interactions is roughly equivalent to that of DOPA–Fe^{3+} crosslinking between mussel coating proteins.[4d,e] Considering the instability of DOPA in oxidative environments, the cation–π interaction can be considered as an alternative cross-linking mechanism for the design and development of underwater adhesives.

Acknowledgements

The work was supported by an NSERC Discovery Grant Award and an NSERC RTI Grant Award from the Natural Sciences and Engineering Research Council of Canada (H. Zeng), the National Research Foundation of Korea Grant (NRF-2011-0007605 & NRF-C1ABA001-2011-0029960) and the Marine Biomaterials Research Center grant from the Ministry of Land, Transport and Maritime Affairs, Korea (D. S. Hwang), and partially supported by Grant NRF-2012R1A1A2009275 and Supercomputing Center/Korea Institute of Science and Technology Information with supercomputing resources including technical support (Y. S. Jho).

Notes and references

1 (*a*) J. H. Waite, *Science*, 1983, **212**, 1038–1040; (*b*) H. Lee, B. P. Lee and P. B. Messersmith, *Nature*, 2007, **448**, 338–341; (*c*) K. Kamino, *Biofouling*, 2013, **29**, 735–749; (*d*) R. J. Stewart, T. C. Ransom and V. Hlady, *J. Polym. Sci., Part B: Polym. Phys.*, 2013, **49**, 757–771; (*e*) J. R. Burkett, L. M. Hight, P. Kenny and J. J. Wilker, *J. Am. Chem. Soc.*, 2010, **132**, 12531–12533; (*f*) E. Hennebert, R. Wattiez, M. Demeuldre, P. Ladurner, D. S. Hwang, J. H. Waite and P. Flammang, *Proc. Natl. Acad. Sci. U. S. A.*, 2014, **111**, 6317–6322.

2 (*a*) J. H. Waite, N. H. Andersen, S. Jewhurst and C. Sun, *J. Adhes.*, 2005, **81**, 297–317; (*b*) B. P. Lee, P. B. Messersmith, J. N. Israelachvili and J. H. Waite, *Annu. Rev. Mater. Res.*, 2011, **41**, 99–132; (*c*) J. H. Waite, *J. Biol. Chem.*, 1983, **258**, 2911–2915; (*d*) H. Lee, N. F. Scherer and P. B. Messersmith, *Proc. Natl. Acad. Sci. U. S. A.*, 2006, **103**, 12999–13003; (*e*) M. J. Sever, J. T. Weisser, J. Monahan, S. Srinivasan and J. J. Wilker, *Angew. Chem., Int. Ed.*, 2004, **43**, 447–450; (*f*) M. Yu, J. Hwang and T. J. Deming, *J. Am. Chem. Soc.*, 1999, **121**, 5825–5826.

3 (*a*) T. J. Deming, *Curr. Opin. Chem. Biol.*, 1999, **3**, 100–105; (*b*) H. G. Silverman and F. F. Roberto, *Mar. Biotechnol.*, 2007, **9**, 661–681.

4 (*a*) J. Yu, W. Wei, R. K. Ashley, J. N. Israelachvili and J. H. Waite, *Nat. Chem. Biol.*, 2012, **7**, 588–590; (*b*) J. Yu, W. Wei, R. K. Ashley, J. N. Israelachvili and J. H. Waite, *Adv. Mater.*, 2011, **23**, 2362–2366; (*c*) W. Wei, J. Yu, C. Broomell, J. N. Israelachvili and J. H. Waite, *J. Am. Chem. Soc.*, 2012, **135**, 377–383; (*d*) H. Zeng, D. S. Hwang, J. H. Waite and J. N. Israelachvili, *Proc. Natl. Acad. Sci. U. S. A.*, 2010, **107**, 12850–12853; (*e*) D. S. Hwang, H. Zeng, A. Masic, M. J. Harrington, J. N. Israelachvili and J. H. Waite, *J. Biol. Chem.*, 2010, **285**, 25850–25858.

5 (*a*) D. S. Hwang, H. Zeng, Q. Lu, J. Israelachvili and J. H. Waite, *Soft Matter*, 2012, **8**, 5640–5648; (*b*) Q. Lu, D. S. Hwang, Y. Liu and H. Zeng, *Biomaterials*, 2012, **33**, 1903–1911.

6 (*a*) D. A. Dougherty, *Science*, 1996, **271**, 163–168; (*b*) J. C. Ma and D. A. Dougherty, *Chem. Rev.*, 1997, **97**, 1303–1324; (*c*) G. Waksman, *et al.*, *Nature*, 1992, **358**, 646–665; (*d*) N. D. Zacharias and A. Dougherty, *Trends Pharmacol. Sci.*, 2002, **23**, 281–287; (*e*) L. M. Salonen, M. Ellermann and F. Diederich, *Angew. Chem., Int. Ed.*, 2011, **50**, 4808–4842; (*f*) P. C. Kearney, L. S. Mizoue, R. A. Kumpf, J. E. Forman, A. McCurdy and D. A. Dougherty, *J. Am. Chem. Soc.*, 1993, **115**, 9907–9919; (*g*) S. Mecozzi, A. P. West Jr and D. A. Dougherty, *J. Am. Chem. Soc.*, 1996, **118**, 2307–2308; (*h*) J. P. Gallivan and D. A. Dougherty, *J. Am. Chem. Soc.*, 2000, **122**, 870–874; (*i*) R. Wu and T. B. McMahon, *J. Am. Chem. Soc.*, 2008, **130**, 12554–12555; (*j*) A. S. Mahadevi and G. N. Sastry, *Chem. Rev.*, 2013, **113**, 2100–2138.

7 (*a*) R. MacKinnon and G. Yellen, *Science*, 1990, **250**, 276–279; (*b*) C. A. Ahern, A. L. Eastwood, H. A. Lester, D. A. Dougherty and R. Horn, *J. Gen. Physiol.*, 2006, **128**, 649–657.

8 (*a*) N. Unwin, *Nature*, 1995, **373**, 37–43; (*b*) J. D. Schmitt, C. G. V. Sharples and W. S. Caldwell, *J. Med. Chem.*, 1999, **42**, 3066–3074.

9 E. V. Pletneva, A. T. Laederach, D. B. Fulton and N. M. Kostić, *J. Am. Chem. Soc.*, 2001, **123**, 6232–6245.

10 C. Mazza, N. Auphan-Anezin, C. Gregoire, A. Guimezanes, C. Kellenberger, A. Roussel, A. Kearney, P. A. Van Der Merwe, A. M. Schmitt-Verhulst and B. Malissen, *EMBO J.*, 2007, **26**, 1972–1983.

11 Q. Lu, D. X. Oh, Y. Lee, Y. Jho, D. S. Hwang and H. Zeng, *Angew. Chem., Int. Ed.*, 2013, **52**, 3944–3948.

12 T. A. D. D. A. Case, T. E. Cheatham III, C. L. Simmerling, J. Wang, R. E. Duke, R. Luo, R. C. Walker, W. Zhang, K. M. Merz, B. Roberts, B. Wang, S. Hayik, A. Roitberg, G. Seabra, I. Kolossváry, K. F. Wong, F. Paesani, J. Vanicek, J. Liu, X. Wu, S. R. Brozell, T. Steinbrecher, H. Gohlke,

Q. Cai, X. Ye, J. Wang, M. J. Hsieh, G. Cui, D. R. Roe, D. H. Mathews, M. G. Seetin, C. Sagui, V. Babin, T. Luchko, S. Gusarov, A. Kovalenko and P. A. Kollman, *AMBER11, Description*, University of California, San Francisco, 2010.

13 G. W. T. M. J. Frisch, H. B. Schlegel, G. E. Scuseria, M. A. Robb, J. R. Cheeseman, G. Scalmani, V. Barone, B. Mennucci, G. A. Petersson, H. Nakatsuji, M. Caricato, X. Li, H. P. Hratchian, A. F. Izmaylov, J. Bloino, G. Zheng, J. L. Sonnenberg, M. Hada, M. Ehara, K. Toyota, R. Fukuda, J. Hasegawa, M. Ishida, T. Nakajima, Y. Honda, O. Kitao, H. Nakai, T. Vreven, J. A. Montgomery Jr, J. E. Peralta, F. Ogliaro, M. Bearpark, J. J. Heyd, E. Brothers, K. N. Kudin, V. N. Staroverov, R. Kobayashi, J. Normand, K. Raghavachari, A. Rendell, J. C. Burant, S. S. Iyengar, J. Tomasi, M. Cossi, N. Rega, J. M. Millam, M. Klene, J. E. Knox, J. B. Cross, V. Bakken, C. Adamo, J. Jaramillo, R. Gomperts, R. E. Stratmann, O. Yazyev, A. J. Austin, R. Cammi, C. Pomelli, J. W. Ochterski, R. L. Martin, K. Morokuma, V. G. Zakrzewski, G. A. Voth, P. Salvador, J. J. Dannenberg, S. Dapprich, A. D. Daniels, Ö. Farkas, J. B. Foresman, J. V. Ortiz, J. Cioslowski and D. J. Fox, *Gaussian09, Description*, Gaussian, Inc, Wallingford CT, 2009.

14 (*a*) J. N. Israelachvili, *et al.*, *Rep. Prog. Phys.*, 2010, **73**, 036601–036617; (*b*) J. N. Israelachvili, *Intermolecular and Surface Forces*, Academic press, revised 3rd edn, 2011.

15 (*a*) M. Kanyalkar, S. Srivastava and E. Coutinho, *Biomaterials*, 2002, **23**, 389–399; (*b*) D. S. Hwang and J. H. Waite, *Protein Sci.*, 2012, **21**, 1689–1695; (*c*) J. Mou, D. M. Czajkowsky, Y. Zhang and Z. Shao, *FEBS Lett.*, 1995, **371**, 279–282.

16 (*a*) M. Valtiner, S. H. Donladon, M. A. Gebbie and J. N. Israelachvili, *J. Am. Chem. Soc.*, 2012, **134**, 1764; (*b*) A. Y. Grosberg, T. T. Nguyen and B. I. ShklovskiiZeng, *Rev. Mod. Phys.*, 2002, **74**, 329–345; (*c*) A. V. Dobrynin and M. Rubinstein, *Prog. Polym. Sci.*, 2005, **30**, 1049–1118.